

# Optical spectra of the silicon-terminated carbon chain radicals $\text{SiC}_n\text{H}$ ( $n = 3,4,5$ )

Cite as: J. Chem. Phys. **141**, 044310 (2014); <https://doi.org/10.1063/1.4883521>

Submitted: 27 February 2014 . Accepted: 03 June 2014 . Published Online: 29 July 2014

D. L. Kokkin, N. J. Reilly, R. C. Fortenberry, T. D. Crawford, and M. C. McCarthy



View Online



Export Citation



CrossMark

## ARTICLES YOU MAY BE INTERESTED IN

**Communication: The ground electronic state of  $\text{Si}_2\text{C}$ : Rovibrational level structure, quantum monodromy, and astrophysical implications**

The Journal of Chemical Physics **142**, 231101 (2015); <https://doi.org/10.1063/1.4922651>

**Rotational spectra of  $\text{SiCN}$ ,  $\text{SiNC}$ , and the  $\text{SiC}_n\text{H}$  ( $n=2, 4-6$ ) radicals**

The Journal of Chemical Physics **115**, 870 (2001); <https://doi.org/10.1063/1.1370068>

**Laser spectroscopy of the  $\tilde{A}2\Sigma^+ - \tilde{X}2\Pi_i$  band system of I-SiC<sub>3</sub>H**

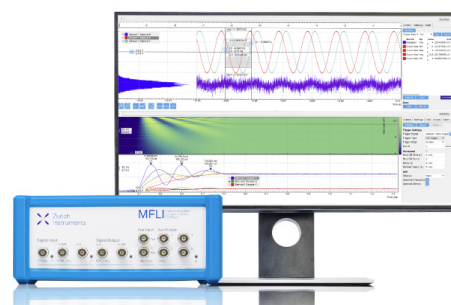
The Journal of Chemical Physics **143**, 174304 (2015); <https://doi.org/10.1063/1.4934785>

## Challenge us.

What are your needs for periodic signal detection?



Zurich  
Instruments



# Optical spectra of the silicon-terminated carbon chain radicals $\text{SiC}_n\text{H}$ ( $n = 3, 4, 5$ )

D. L. Kokkin,<sup>1,2,a)</sup> N. J. Reilly,<sup>1,2,b)</sup> R. C. Fortenberry,<sup>3,c)</sup> T. D. Crawford,<sup>3</sup>  
 and M. C. McCarthy<sup>1,2,d)</sup>

<sup>1</sup>Harvard-Smithsonian Center for Astrophysics, Cambridge, Massachusetts 02138, USA

<sup>2</sup>School of Engineering and Applied Sciences, Harvard University, 29 Oxford St., Cambridge, Massachusetts 02138, USA

<sup>3</sup>Department of Chemistry, Virginia Tech, Blacksburg, Virginia 24061, USA

(Received 27 February 2014; accepted 3 June 2014; published online 29 July 2014)

The gas-phase optical spectra of three silicon-terminated carbon chain radicals,  $\text{SiC}_n\text{H}$  ( $n = 3 - 5$ ), formed in a jet-cooled discharge of silane and acetylene, have been investigated by resonant two-color two-photon ionization and laser-induced fluorescence/dispersed fluorescence. Analysis of the spectra was facilitated by calculations performed using equation-of-motion coupled cluster methods. For  $\text{SiC}_3\text{H}$  and  $\text{SiC}_5\text{H}$ , the observed transitions are well-described as excitations from a  $^2\Pi$  ground state to a  $^2\Sigma$  state, in which vibronic coupling, likely involving a higher-lying  $\Pi$  state with a very large predicted  $f$ -value (close to unity), is persistent. The lowest  $^2\Sigma$  states of both species are characterized by a rare silicon triple bond, which was identified previously [T. C. Smith, H. Y. Li, D. J. Clouthier, C. T. Kingston, and A. J. Merer, *J. Chem. Phys.* **112**, 3662 (2000)] in the lowest  $^2\Sigma$  state of  $\text{SiCH}$ . Although a strong  $\Pi - \Pi$  transition is predicted for  $\text{SiC}_4\text{H}$ , the observed spectrum near 505 nm more likely corresponds to excitation to a relatively dark  $\Sigma$  state which is vibronically coupled to a nearby  $\Pi$  state. In contrast to the chains with an odd number of carbon atoms, which exhibit relatively sharp spectral features and lifetimes in the 10–100 ns range,  $\text{SiC}_4\text{H}$  shows intrinsically broadened spectral features consistent with a  $\sim 100$  fs lifetime, and a subsequent long-lived decay ( $> 50 \mu\text{s}$ ) which we ascribe to mixing with a nearby quartet state arising from the same electronic configuration. The spin-orbit coupling constants for both  $\text{SiC}_3\text{H}$  and  $\text{SiC}_5\text{H}$  radicals were determined to be approximately  $64 \text{ cm}^{-1}$ , similar to that of  $\text{SiCH}$  ( $69.8 \text{ cm}^{-1}$ ), suggesting that the unpaired electron in these species is localized on the silicon atom. Motivated by the new optical work, the rotational spectrum of linear  $\text{SiC}_3\text{H}$  was detected by cavity Fourier-transform microwave spectroscopy in the 13–34 GHz range. Each rotational transition from the  $^2\Pi_{3/2}$  ground state exhibits well-resolved  $\Lambda$ -doubling and hyperfine structure; the derived rotational constant of  $B = 2.605 \text{ GHz}$  is in excellent agreement with our calculations. © 2014 AIP Publishing LLC. [<http://dx.doi.org/10.1063/1.4883521>]

## I. INTRODUCTION

Both silicon and carbon are among the most abundant elements in circumstellar and interstellar environments and thus play vital roles in astrochemical processes. The carbon chain is a persistent structural motif among interstellar molecules: many hydrogen-terminated carbon chains ( $\text{C}_n\text{H}$ ), including both neutral and ionized species, have been observed in a variety of astronomical sources.<sup>1,2</sup> Because small silicon-containing species are also quite conspicuous in circumstellar shells of certain evolved carbon stars, silicon-substituted analogues of known or postulated carbon chains may be plausible targets for astronomical detection; they are also likely to be highly polar and possess conjugated structures, implying that they have strong electronic transitions in the visible region of

the spectrum. For these reasons, appropriately “doped” carbon chains are attractive as potential carriers of the elusive diffuse interstellar bands (DIBs),<sup>3</sup> for which carbon chains have been proposed as viable candidates (see, for example, Ref. 4 and references therein).

Motivated by this possibility, several silicon-terminated carbon chain radicals of the form  $\text{SiC}_n\text{H}$  ( $n = 2, 4 - 6$ ), were identified in a jet-cooled silane-acetylene discharge by Fourier-transform microwave (FTMW) spectroscopy.<sup>5</sup> All were determined to have linear or nearly linear geometries with  $^2\Pi$  ground states and exhibited well-resolved hyperfine structure, with regular ( $^2\Pi_{1/2}$  lowest in energy) and inverted ( $^2\Pi_{3/2}$  lowest) rotational ladders for  $n$  even and odd, respectively. While it should also have been possible to detect the rotational spectrum of the missing member of the series –  $\text{SiC}_3\text{H}$  – searches for its transitions were unsuccessful.

In light of the non-detection of the linear  $\text{SiC}_3\text{H}$  isomer, Sun *et al.* predicted in a recent theoretical study that several stable ring isomers should lie close in energy to the linear ground state, including a rhomboidal structure, located 11.2 kcal/mol above ground, in which the hydrogen atom

<sup>a)</sup>Current address: Department of Chemistry and Biochemistry, Arizona State University, Tempe, Arizona 85287, USA.

<sup>b)</sup>Current address: Department of Chemistry, University of Louisville, Louisville, Kentucky 40292, USA.

<sup>c)</sup>Current address: Department of Chemistry, Georgia Southern University, Statesboro, Georgia 30460, USA.

<sup>d)</sup>Author to whom correspondence should be addressed. Electronic mail: [mccarthy@cfa.harvard.edu](mailto:mccarthy@cfa.harvard.edu)

is bonded *para* to silicon.<sup>6</sup> Both linear and rhomboidal isomers of SiC<sub>3</sub>, as well as highly energetic isomers of other species – notably isofulminic acid (HONC), lying 84 kcal/mol above ground – have been detected using the same discharge source,<sup>7–9</sup> so it is not unreasonable to posit that energetic isomers of SiC<sub>3</sub>H could be efficiently formed in the silane/acetylene discharge; however, the non-detection of the linear isomer remained surprising.

The electronic spectra of many C<sub>*n*</sub>H chains have now been studied in connection with the DIBs using fluorescence, absorption (cavity ring-down), and mass-selective techniques.<sup>10</sup> By analogy with the C<sub>4</sub>H and C<sub>6</sub>H radicals, which exhibit fairly strong, well-resolved transitions in the visible region to excited states of Π symmetry (origin bands at 420 nm<sup>11</sup> and 526 nm,<sup>12</sup> respectively), it was suggested<sup>5</sup> that the isovalent *l*-SiC<sub>3</sub>H and *l*-SiC<sub>5</sub>H radicals should be good candidates for optical detection. In contrast to the well-characterized carbon chains, however, almost no optical data exists for the silicon-bearing radicals, the sole exception being the shortest member in the series, SiCH, whose  $\tilde{X}^2\Pi_i$  transition was first observed in emission by Cireasa and Cossart<sup>13</sup> in a discharge through a flowing mixture of hexamethyldisilane and helium. This transition was subsequently investigated in the region 600–815 nm by Smith *et al.* using laser-induced fluorescence.<sup>14</sup> Detailed analysis of the rotationally resolved electronic spectrum yielded the first ever identification of a silicon triple bond – in the first excited state, which has Σ symmetry – with a bond length of  $\approx 1.61$  Å; in contrast, the triply bonded Σ state of isovalent CCH lies significantly below (by nearly 0.5 eV<sup>15</sup>) the excited Π state.

The unusual bonding in the excited state of SiCH in comparison to CCH serves to emphasize that, beyond their relevance to astrophysics, the investigation of such systems has intrinsic fundamental value in elucidating differences in bonding and electronic structure between carbon and silicon. In this paper, we report the optical spectra of the silicon-terminated carbon chains SiC<sub>3</sub>H, SiC<sub>4</sub>H, and SiC<sub>5</sub>H, produced in a jet-cooled discharge of silane and acetylene, by means of resonant two-color two-photon ionization (R2PI) spectroscopy. Laser-induced fluorescence and dispersed fluorescence spectra were recorded for SiC<sub>3</sub>H to confirm that the observed isomer has a linear geometry (the other chains are not amenable to fluorescence detection). Interpretation of the spectra has been facilitated by calculations of the ground and several excited states of SiC<sub>*n*</sub>H radicals (for *n* = 3 – 6) using coupled cluster and equation-of-motion coupled-cluster (EOM-CC) methods. Motivated by the new optical data and high-level quantum chemical calculations, the rotational spectrum of *l*-SiC<sub>3</sub>H has now been observed by FTMW spectroscopy in the 13–34 GHz range, and precise spectroscopic constants derived for its  $^2\Pi_{3/2}$  ground state.

## II. EXPERIMENTAL DETAILS

The silicon-terminated carbon chains (SiC<sub>*n*</sub>H) were produced by applying an electric discharge to a 1%SiH<sub>4</sub>/1%C<sub>2</sub>H<sub>2</sub>/Ar premix during the early stages of adiabatic expansion into a large source chamber (typical pressure with the gas expanding is  $3 \times 10^{-6}$  Torr). The expansion was

skimmed 50 mm downstream by a 2 mm skimmer prior to passing into a differentially pumped extraction chamber (typical operating pressure  $10^{-7}$  Torr). The skimmed beam was then probed between the extraction grids via a two color scheme, in which the resonant photon was produced by a Nd:YAG-pumped dye laser which operates in the 390–700 nm range. The resulting electronically excited molecules were subsequently ionized using 193 nm radiation from an excimer laser containing Ar/F<sub>2</sub> premix. The power of the excimer laser was adjusted such that non-resonant ion signal during scans was minimized. Each spectrum required the use of several laser dyes; while no attempt was made to normalize for laser power, the output was kept approximately constant  $\sim 10$  mJ per pulse throughout the entire 390–700 nm range by mixing overlapping dye solutions and/or adjusting the pump laser power as necessary. While the pure carbon chains C<sub>*n*</sub>H often exhibit origin-dominated transitions,<sup>16,17</sup> the origin band of SiC<sub>3</sub>H was relatively weak when 193 nm was used as the ionizing wavelength, leading us to suspect that ionization was occurring near threshold. Indeed, the relative strength of this band increased by a factor of almost two when higher energy 157 nm (F<sub>2</sub>) radiation was used instead. No such dependence was observed for the longer chains, both of which have lower IPs and whose origin bands occur at higher energies.

Laser-induced fluorescence/dispersed fluorescence (LIF/DF) studies were undertaken in a separate experimental apparatus to determine ground state vibrational frequencies for comparison with calculations. In this experiment, jet-cooled SiC<sub>3</sub>H was generated using the same gas premix and pulsed discharge source, and laser-induced fluorescence was imaged by *f*/1 optics and detected using a monochromator equipped with a photomultiplier tube (PMT). A small (14 cm) monochromator was used as a broad bandpass filter (FWHM 30 nm) during excitation scans to limit spectral contamination from metastable Ar and other abundant discharge products, notably C<sub>2</sub> and Si<sub>2</sub>, which have strong transitions throughout this region.<sup>18,19</sup> For DF, a 1 m monochromator was operated with 0.5 mm slits to record moderate resolution emission spectra (FWHM  $\sim 30$  cm<sup>-1</sup>) from electronically excited SiC<sub>3</sub>H in the vibrationless level and the two lowest excited vibronic levels. A cursory search for SiC<sub>5</sub>H by LIF/DF was unsuccessful, presumably owing to the much shorter lifetime of the upper state –  $\sim 10$  ns, compared to 100 ns for SiC<sub>3</sub>H – which is comparable to the rise-time of the PMT used in this work (lifetimes were estimated by adjusting the time delay between the tunable and ionizing photons in R2PI). The SiC<sub>4</sub>H spectrum appears to be intrinsically broadened and thus is not a good target for LIF detection; no obvious decay in R2PI signal for SiC<sub>4</sub>H was observed even when the ionization laser was delayed by 50 μs relative to the tunable radiation, possibly indicating mixing with a quartet state.

A renewed search for rotational transitions of linear SiC<sub>3</sub>H was undertaken concurrently with the optical spectroscopy with the same FTMW spectrometer and discharge nozzle source as that used in our earlier work on silicon-terminated carbon chains.<sup>5</sup> Prior to undertaking the new search, the experimental conditions were optimized to produce SiC<sub>4</sub>H in high yield. Lines of SiC<sub>4</sub>H were observed

most intensely in a mixture of 0.1%SiH<sub>4</sub>/0.2%C<sub>2</sub>H<sub>2</sub> diluted in neon, and a voltage of 1 kV delivered to the inner electrode (closest to the valve orifice) of the discharge nozzle. SiC<sub>3</sub>H has a <sup>2</sup>Π<sub>3/2</sub> ground state with a large magnetic *g* factor, which causes its low-*J* rotational transitions to be easily split or broadened by even a small Zeeman field; for this reason, a search for a relatively high *J* transition (*J* = 11/2 – 9/2) was undertaken first. The search range covered ±1% in frequency of our best estimate, which was determined by scaling our calculated rotational constant by the ratio between that predicted (based on the same calculations) and measured (from Ref. 5) for SiC<sub>3</sub>H.

### III. COMPUTATIONAL DETAILS

Ground state geometries were optimized utilizing coupled cluster singles, doubles, and perturbative triples [CCSD(T)]<sup>20</sup> making use of unrestricted Hartree-Fock reference wavefunctions (UHF)<sup>21,22</sup> with Dunning and co-workers' cc-pVTZ basis set<sup>23,24</sup> with silicon utilizing the cc-pV(T+d)Z basis set<sup>25</sup> simply called cc-pVTZ from here on. Computations of vertical excitation energies and oscillator strengths from these CCSD(T)/cc-pVTZ geometries were carried out at the CCSD level of theory<sup>26</sup> as well as energies with the approximate, iterative triples CC3 method<sup>27–30</sup> in the EOM formalism<sup>31,32</sup> using augmented forms of the aforementioned Dunning triple-zeta basis sets<sup>25,33</sup> and restricted open-shell reference (ROHF) wavefunctions<sup>34–37</sup> previously shown to provide superior treatment of excited states of closely related linear carbon radicals.<sup>38</sup>

Building from earlier studies involving excited states of silicon-containing interstellar molecules,<sup>39–41</sup> adiabatic excitation energies were computed from the energy differences between the optimized forms of the ROHF-CCSD/aug-cc-pVTZ ground and ROHF-EOM-CCSD/aug-cc-pVTZ

excited state geometries. Harmonic vibrational frequencies were computed via finite differences of energies for each geometry which allowed for further refinement of the adiabatic excitation energies for zero-point vibrational energy (ZPE) corrections.<sup>42</sup> All computations of the linear radicals were undertaken in the C<sub>2v</sub> point group, the largest Abelian subgroup of C<sub>∞v</sub>. The PSI3 suite of computational chemistry programs<sup>43</sup> was used for all of the computations, with the exception of the ⟨*s*<sup>2</sup>⟩ expectation values, which were calculated with the CFOUR quantum chemistry package.<sup>44</sup>

## IV. RESULTS

### A. Computational results

The SiC<sub>*n*</sub>H radicals have <sup>2</sup>Π ground states as determined by rotational spectroscopy,<sup>5</sup> but the electronic configurations differ between two subclasses. Chains with an odd number of carbon atoms have three electrons in the π highest occupied molecular orbital (HOMO) while only one electron is present in the π HOMO for the chains with an even number of C atoms. Thus, SiC<sub>3</sub>H has an electronic configuration of (core)10σ<sup>2</sup> 2π<sup>4</sup> 11σ<sup>2</sup> 3π<sup>3</sup>, and SiC<sub>5</sub>H is (core)14σ<sup>2</sup> 2π<sup>4</sup> 15σ<sup>2</sup> 3π<sup>4</sup> 4π<sup>3</sup>, whereas SiC<sub>4</sub>H is (core)11σ<sup>2</sup> 12σ<sup>2</sup> 2π<sup>4</sup> 13σ<sup>2</sup> 3π<sup>4</sup> 4π<sup>1</sup>. Similar electronic configurations have been noted for the analogous carbon chains, including those with more than four heavy atoms.<sup>10,38,45</sup> Rotational constants derived from the optimized geometries (Table II) of each chain are in excellent agreement (<1.3%) with those obtained in the earlier microwave work,<sup>5</sup> and with the new microwave data on SiC<sub>3</sub>H reported herein (see Sec. IV B 2).

The calculations indicate that chains within the respective isovalent odd and even *n* groupings have similar electronic excitation behavior. As listed in Table I, the strongest optical

TABLE I. Excitation energies (in eV) for the first few states of the <sup>2</sup>Π SiC<sub>*n*</sub>H radicals (*n* = 3 – 6) from coupled cluster aug-cc-pVTZ computations.

Molecule	State	⟨ <i>s</i> <sup>2</sup> ⟩	Excitation character	Vertical			Adiabatic		Expt.
				CCSD	<i>f</i>	CC3	CCSD	ZPE-CCSD	
SiC <sub>3</sub> H	1 Σ <sup>+</sup>	0.839	11σ → 3π (0.88 β)	2.19	0.003	1.98	2.04	2.08	1.83
	2 Π	2.799	3π → 4π*	2.50	10 <sup>-5</sup>	2.51	...	...	...
			3π → 5π*	(0.39 β; 0.30 α)					
SiC <sub>4</sub> H	3 Π	3.320	4π → 5π*	5.36	1.06	...	...	...	...
			13σ → 4π	2.66	10 <sup>-5</sup>	2.54	...	...	2.45
	2 Π	2.707	4π → 4π 13σ → 4π	(0.64 β; 0.59 α)					
3π → 4π			3.18	0.012	3.06	2.84	2.73	...	
3π → 4π			(0.43 β; 0.41 α)						
SiC <sub>5</sub> H	2 Π	2.707	4π → 7π*	(0.31 β)					
			4π → 5π*	(0.25 α)					
			4π → 6π*	(0.63 β; 0.47 α)	2.25	10 <sup>-6</sup>	2.25	...	...
SiC <sub>6</sub> H	1 Σ <sup>+</sup>	0.856	4π → 7π*	(0.30 β; 0.23 α)					
			15σ → 4π	2.29	0.003	2.07	2.12	2.16	1.94
			2π → 5π*	4.91	0.68	...	...	...	...
SiC <sub>6</sub> H	1 <sup>2</sup> Σ <sup>-</sup>		17σ → 5π	(0.89 β)	2.68	10 <sup>-5</sup>	2.56	...	...
			5π → 5π 17σ → 5π	(0.64 β; 0.58 α)					
			4π → 5π	(0.20 αβ)					
			4π → 5π	(0.40 β; 0.36 α)	2.71	0.015	2.57	...	...
2 <sup>2</sup> Π			4π → 5π	(0.28 β)					
			4π → 5π	(0.26 α)					
			5π → 7π*						

TABLE II. Bond lengths (in Å) and rotational constants  $B$  (in MHz, with experimental values from Ref. 5 and the present work in parentheses beneath) for relevant electronic states of  $\text{SiC}_n\text{H}$  ( $n = 3 - 6$ ) from CCSD and EOM-CCSD calculations with an aug-cc-pVTZ basis.

Molecule	Parameter	Electronic state		
		$1^2\Pi$	$1^2\Sigma^+$	$2^2\Pi$
$\text{SiC}_3\text{H}$	Si-C1	1.692	1.611	1.853
	C1-C2	1.351	1.38	1.307
	C2-C3	1.225	1.211	1.251
	C3-H	1.062	1.062	1.063
	$B$	2594.70 (2605.0528)	2675.95	2427.12
$\text{SiC}_4\text{H}$	Si-C1	1.805	1.781	1.774
	C1-C2	1.231	1.22	1.303
	C2-C3	1.372	1.376	1.305
	C3-C4	1.21	1.209	1.256
	C4-H	1.063	1.062	1.063
	$B$	1398.23 (1415.7035)	1415.92	1392.24
$\text{SiC}_5\text{H}$	Si-C1	1.693	1.613	
	C1-C2	1.334	1.373	
	C2-C3	1.236	1.215	
	C3-C4	1.362	1.376	
	C4-C5	1.213	1.209	
	C5-H	1.062	1.062	
	$B$	878.69 (883.8539)	890.98	
$\text{SiC}_6\text{H}$	Si-C1	1.801		
	C1-C2	1.234		
	C2-C3	1.363		
	C3-C4	1.216		
	C4-C5	1.374		
	C5-C6	1.209		
	$B$	571.40 (578.1810)		

transition of the odd- $n$  chains is dominated by a single excitation from the  $\sigma$  HOMO-1 into the  $\pi$  HOMO creating a filled  $\pi$  orbital and a  $^2\Sigma^+$  excited state. In contrast, the even  $n$  radicals do not have appreciably strong transitions to a  $\Sigma^+$  state; instead, their visible spectra are predicted to be dominated by transitions to a  $\Pi$  state. These  $\Pi - \Pi$  transitions are primarily composed of transitions out of the fully occupied  $\pi$  HOMO-1 into the singly occupied  $\pi$  HOMO (the second-highest occupied molecular orbital or SHOMO), though excitations out of the SHOMO into higher  $\pi^*$  orbitals also contribute to the overall excitation character.

The differences in excitation character for the two subclasses are reflected in geometry changes upon excitation. As indicated in Table II, a commonality between  $\text{SiC}_3\text{H}$  and  $\text{SiC}_5\text{H}$  is that the major changes in bond length are confined to the Si-C-C moiety, with a significant shortening (by 0.08 Å) of the Si-C bond upon excitation to create a nominal Si-C triple bond, while the neighboring C-C bond length increases slightly. Alternation in the C-C bond lengths in the ground state becomes more pronounced in the excited state. The net result for both is that the overall chain length decreases

slightly upon excitation, with an accompanying increase in the rotational constant of a few percent; indeed, this behavior was confirmed experimentally for  $\text{SiCH}$ .<sup>14</sup> For the excited  $\Pi$  state of  $\text{SiC}_4\text{H}$ , the Si-C bond length decreases less markedly, while large ( $>0.05$  Å), alternating increases/decreases in adjacent C-C bond lengths give an excited state that is essentially cumulenic, with a rotational constant that decreases very slightly with respect to the ground state geometry. Such differences are reflected in the experimental spectra: the odd- $n$  spectra show conspicuous activity in the Si-C stretch and Si-C-C bending modes, while the strongest features in the  $\text{SiC}_4\text{H}$  spectrum are due to modes involving the carbon chain.

## B. $\text{SiC}_3\text{H}$

### 1. Optical data

*a. Identification of spectral carrier.* Figure 1 shows the electronic spectrum recorded for  $m/z = 65$  in the region 14 500–16 500  $\text{cm}^{-1}$ . To confirm that the carrier contained silicon, the measurement was repeated using a discharge of pure acetylene, and as expected, none of the same spectral features were observed. The band at 197  $\text{cm}^{-1}$  relative to the origin is close to the lowest bending frequency observed in the isovalent  $\text{C}_4\text{H}$  carbon chain (189  $\text{cm}^{-1}$  for the  $\tilde{B}$  state<sup>11</sup> and at 220  $\text{cm}^{-1}$  for the  $\tilde{A}$  state<sup>46,47</sup>), giving some confidence that the structure of the  $\text{SiC}_3\text{H}$  radical detected here is also a linear chain. Additionally, a frequency of 165  $\text{cm}^{-1}$  is predicted for the SiCC bend of linear  $\text{SiC}_3\text{H}$  (in the ground state) by Sun *et al.*<sup>6</sup> However, owing to the earlier non-detection of this isomer by microwave spectroscopy, and to the number of low-lying nonlinear  $\text{SiC}_3\text{H}$  isomers predicted by theory,<sup>6</sup> LIF-DF spectroscopy was needed to firmly establish that the observed spectrum arises from the linear form.

A portion of the LIF spectrum containing the origin and several higher vibronic bands, compared to the R2PI spectrum, is shown in Fig. 2. The signal-to-noise (S/N) ratio is significantly worse than in the R2PI spectrum owing to both the short fluorescence lifetime (making rejection of scattered laser light difficult), and measures taken to reduce spectral interference by the  $\text{C}_2$  Swan bands,<sup>18</sup> as well as  $\text{Si}_2$ <sup>19</sup> (a low discharge voltage, in comparison to the R2PI experiment, and a large nozzle-laser distance were required to prevent vibrationally and rotationally hot  $\text{Si}_2$  and  $\text{C}_2$  from obscuring the  $\text{SiC}_3\text{H}$  spectrum). Nevertheless, the LIF spectrum shows several clear coincidences with the R2PI spectrum recorded at  $m/z = 65$ , strongly suggesting that these features are good targets for further study by DF spectroscopy.

DF spectra recorded from the three lowest observed vibrational levels of electronically excited  $\text{SiC}_3\text{H}$  are shown in Fig. 3. For the purpose of identifying the structure of  $\text{SiC}_3\text{H}$  (the spectra are discussed in more detail in Sec. IV B 1 b), it suffices to note that the origin DF spectrum is dominated by a single feature at a Stokes-shift of 64  $\text{cm}^{-1}$ , which cannot be plausibly assigned to a vibrational mode of any isomer calculated by Sun *et al.*<sup>6</sup> Rather, the only sensible assignment of this feature is to the upper spin-orbit component of the  $\Pi$  ground state of the linear chain. A value of 64  $\text{cm}^{-1}$  for  $A_{\text{so}}$  is

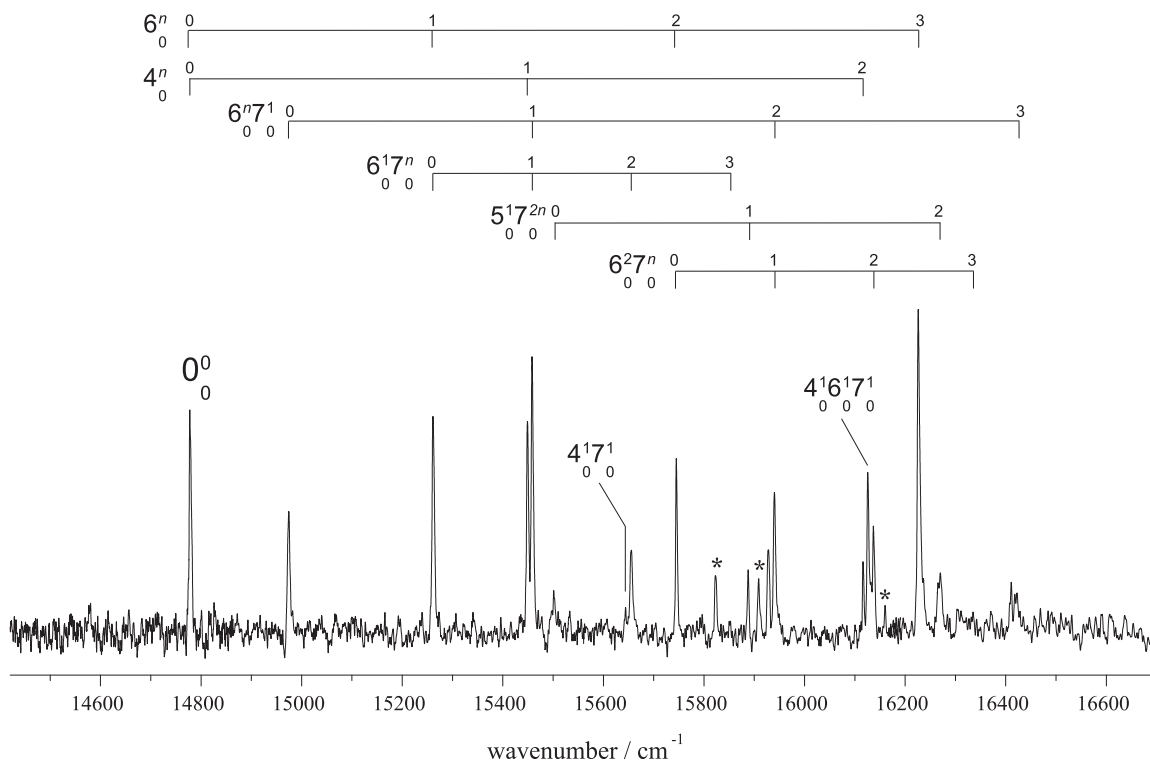


FIG. 1. R2PI spectrum of  $\text{SiC}_3\text{H}$  from an acetylene-silane discharge. Assignments are for the linear chain; features designated with asterisks are presently unassigned and may belong to another isomer.

consistent with that reported for  $\text{SiCH}$  ( $69.8 \text{ cm}^{-114}$ ),  $\text{SiC}_2\text{H}$  ( $72.3 \text{ cm}^{-148}$ ), and that derived herein for  $\text{SiC}_5\text{H}$  ( $64 \text{ cm}^{-1}$ ; see Sec. IV D). The stark contrast between the excitation spectrum – containing strong transitions involving several vibrational modes – and the emission spectrum – which is dominated by a single feature – suggests a fairly vertical transition in which off-diagonal vibrational transitions are largely brought about by vibronic coupling.

*b. Spectral assignment.* With confirmation that the observed spectrum arises from – or at least, is dominated by – the linear isomer, it is possible to proceed with an assignment based on the predicted transition energies,  $f$ -values, and vibrational frequencies given in Tables I and II. Owing to its comparatively high oscillator strength and close agreement between experimental and calculated excitation energies, it is reasonable to assume that the  $\Sigma$  state dominates the observed

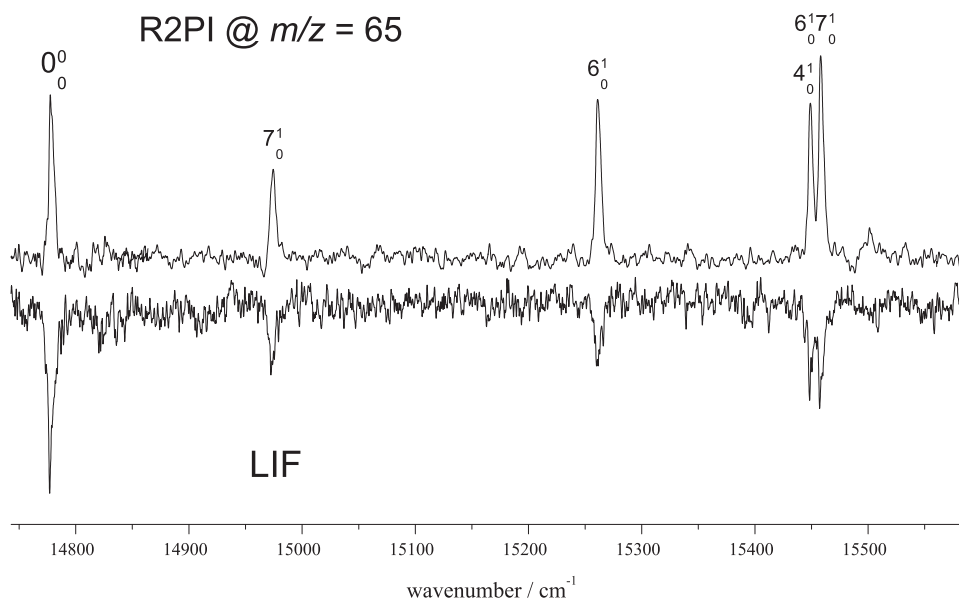


FIG. 2. Comparison between the laser-induced fluorescence and R2PI spectra (recorded at  $m/z = 65$ ) of a silane-acetylene discharge. Intensity discrepancies between the two spectra result primarily from the bandpass used for fluorescence detection.

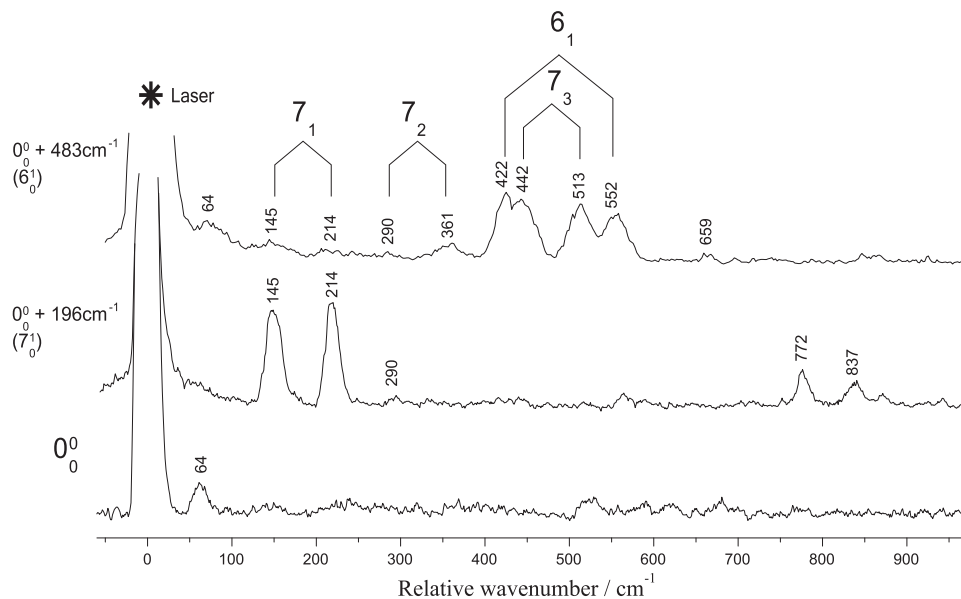


FIG. 3. Dispersed fluorescence spectra from the  $0_0^0$ ,  $7_0^1$  (Si–C–C bend), and  $6_0^1$  (C–C–C bend) levels of the  $1^2\Sigma$  state of  $\text{SiC}_3\text{H}$  radical.

transition. As indicated in Fig. 1 and Table III, it is fairly straightforward to assign a large fraction of the observed bands to harmonic combinations involving a few vibrational modes with fundamental frequencies of  $197\text{ cm}^{-1}$ ,  $483\text{ cm}^{-1}$ , and  $672\text{ cm}^{-1}$ , which we ascribe to the SiCC and CCC bends and the Si–C stretch, respectively; the agreement with the predicted frequencies for these modes in the  $\Sigma$  state is compelling. In this assignment, both Herzberg-Teller-induced transitions and Franck-Condon-allowed transitions are present, reminiscent of the electronic spectrum of isovalent  $\text{C}_4\text{H}$ . Although an electronic state of  $\Pi$  symmetry is predicted to lie nearby (at 2.5 eV), the  $f$ -value for excitation to this state ( $10^{-5}$ ) is almost certainly too small to explain the persistent vibronic coupling throughout the observed spectrum; rather, we believe that a higher-lying  $\Pi$ -state with an extremely strong predicted transition ( $f = 1.026$  at 5 eV) is implicated. This conclusion is supported by EOM-CCSD computations of oscillator strengths at Si–C–C bond angles from  $180^\circ$  to  $95^\circ$ . While both the  $\Sigma$  and higher-lying  $\Pi$  transitions decrease in strength by a factor of several over this range, the latter transition remains at least two orders of magnitude stronger, while the transition strength to the lower  $\Pi$ -state near 2.5 eV remains negligible.

Weak features designated with asterisks – at 1046, 1132, and  $1383\text{ cm}^{-1}$  above the origin – have no obvious assignment to the  $\Sigma$  state of  $\text{SiC}_3\text{H}$ . In this light, an alternative explanation is that the excited state of the observed transition is in fact the nearby  $\Pi$  state, which can be coupled to the brighter  $\Sigma$  state by  $\pi$  vibrational modes, and would have a richer spectrum owing to the Renner-Teller effect (potentially explaining the unassigned bands). We reject this notion, because (1) if it were true, one would expect to see the stronger  $\Sigma - \Pi$  transition nearby; (2) with the exception of those few weak bands, the spectrum has a straightforward assignment in terms of harmonic combinations, reflecting the relative simplicity one tends to expect of a  $\Sigma$  state; (3) several

TABLE III. Excited state band positions (in  $\text{cm}^{-1}$ ) and assignments for  $\text{SiC}_3\text{H}$ . Frequencies are given relative to the origin band at  $14\,778\text{ cm}^{-1}$ .

Frequency	Assignment
0	$0_0^0$
197	$7_0^1$
415	
462	
484	$6_0^1$
563	
672	$4_0^1$
681	$6_0^1 7_0^1$
724	$5_0^1$
869	$4_0^1 7_0^1$
878	$6_0^1 7_0^2$
967	$6_0^2$
1045	
1110	$5_0^1 7_0^2$
1131	
1150	$4_0^1 6_0^1$
1163	$6_0^2 7_0^1$
1201	
1339	$4_0^2$
1348	$4_0^1 6_0^1 7_0^1$
1359	$6_0^2 7_0^2$
1383	
1448	$6_0^3 + 3_0^1$
1492	$5_0^1 7_0^4$
1634	
1641	$6_0^3 7_0^1$
1645	$6_0^3 7_0^1$

TABLE IV. Vibrational energies (in  $\text{cm}^{-1}$ , from Fig. 3) and assignments for the  $\tilde{X}^2\Pi_i$  ground state of  $\text{SiC}_3\text{H}$ .

Vibrational energy ( $\text{cm}^{-1}$ )	Assignment
0	$0_0^0$ ( $^2\Pi_{1/2}$ )
64	( $^2\Pi_{3/2}$ )
145	$7_1$ ( $\mu$ $^2\Sigma_{1/2}$ )
214	$7_1$ ( $\kappa$ $^2\Sigma_{1/2}$ )
290	$7_2$ ( $\mu$ $^2\Pi_{1/2}$ )
360	$7_2$ ( $\kappa$ $^2\Pi_{3/2}$ )
422	$6_1$ ( $\mu$ $^2\Sigma_{1/2}$ )
440	$7_3$ ( $\mu$ $^2\Sigma_{1/2}$ )
510	$7_3$ ( $\kappa$ $^2\Sigma_{1/2}$ )
552	$6_1$ ( $\kappa$ $^2\Sigma_{1/2}$ )
659	$7_4$ ( $\mu$ $^2\Pi_{1/2}$ )
772	$4_1 7_1$ ( $\mu$ $^2\Sigma_{1/2}$ )
837	$4_1 7_1$ ( $\kappa$ $^2\Sigma_{1/2}$ )

of the derived vibrational frequencies are in excellent agreement with the prediction for the  $\Sigma$  state; and (4) the Si–C bond length is predicted to increase significantly (0.11 Å) in the  $\Pi$  state, which would result in a reduced frequency for the Si–C stretch; in contrast, the Si–C stretch frequency increases upon excitation (see further discussion of DF spectra below), which is consistent with the prediction for the  $\Sigma$  state. On the basis of this analysis, we conjecture that these weak unassigned features belong to a different isomer (see Sec. VB).

Because our spectral resolution is insufficient to determine band types, and thereby distinguish upper state levels possessing  $\Sigma$  or  $\Pi$  vibronic symmetry, we use DF spectroscopy to seek qualitative insight into the vibronic bands at  $197\text{ cm}^{-1}$  and  $483\text{ cm}^{-1}$  above the origin. Ground state vibrational assignments are presented in Table IV. The spectrum from the  $197\text{ cm}^{-1}$  level (Fig. 3) has a fairly simple interpretation, because it is dominated by a pair of features located at  $145\text{ cm}^{-1}$  and  $214\text{ cm}^{-1}$ . Both are in reasonable agreement with the predicted  $\nu_7$  (SiCC bend)  $\pi_x$  and  $\pi_y$  frequencies ( $153\text{ cm}^{-1}$  and  $168\text{ cm}^{-1}$ ), which are harmonic frequencies calculated with the unpaired electron forced into the  $\pi_x$  or  $\pi_y$  system (Table V); the small difference between the  $\pi_x$  and  $\pi_y$  vibrational frequencies suggests a small Renner-Teller interaction for this mode ( $\pi_x$  and  $\pi_y$  frequencies are degenerate in the absence of coupling with orbital angular momentum). The separation between the experimental bands ( $69\text{ cm}^{-1}$ ) is also very close to the spin-orbit splitting ( $64\text{ cm}^{-1}$ ) in the origin DF spectrum. The term symbols for vibronic levels of a  $^2\Pi$  state take the form  $^{2S+1}K_P$ , where  $K = |\Lambda + l|$  and  $P = |\Lambda + l + \Sigma|$ . According to an expression from Hougen,<sup>49</sup> when the Renner-Teller interaction is small, the two  $^2\Sigma_{1/2}$  levels corresponding to  $l = \pm 1$  are separated by approximately  $\sqrt{A_{\text{eff}}^2 + \epsilon^2\omega^2(\nu + 1)^2}$ , where  $A_{\text{eff}}$  is an effective spin-orbit coupling constant. Thus, the observed separation is consistent with that expected from spin-orbit, and yields a Renner parameter of order  $\epsilon_7 \sim 0.07\text{ cm}^{-1}$ . Additionally, be-

cause  $197\text{ cm}^{-1}$  is close to the calculated  $\nu_7$  frequency in the  $\Sigma$ -state ( $207\text{ cm}^{-1}$ ), we assign the  $197\text{ cm}^{-1}$  feature as the Herzberg-Teller-induced  $7_0^1$  transition. We interpret the features in the DF spectrum at  $770\text{ cm}^{-1}$  and  $833\text{ cm}^{-1}$  (also separated by approximately  $A_{\text{so}}$ ) similarly: as combinations of the two  $\nu_7$  RT-components with the Si–C stretch ( $\nu_4$ ), yielding a Si–C stretch frequency ( $627\text{ cm}^{-1}$ ) in excellent agreement with theory ( $632\text{ cm}^{-1}$ ), and significantly smaller than the corresponding frequency in the excited state ( $672\text{ cm}^{-1}$ ), as predicted.

The transition at  $0_0^0 + 483\text{ cm}^{-1}$  can also be assigned as a Herzberg-Teller-induced transition to the CCC bend ( $\nu_6$ ). Because  $\nu_7$  has a very small Renner-Teller splitting, its transitions should be fairly harmonic; indeed, bands can be found near  $290\text{ cm}^{-1}$  and  $360\text{ cm}^{-1}$  (2 quanta) and  $440\text{ cm}^{-1}$  and  $510\text{ cm}^{-1}$  (three quanta). We therefore assign the remaining strong bands, at  $422\text{ cm}^{-1}$  and  $552\text{ cm}^{-1}$ , as the lower ( $\mu$   $^2\Sigma_{1/2}$ ) and upper ( $\kappa$   $^2\Sigma_{1/2}$ ) components of  $\nu_6$ , respectively. This assignment gives a zeroth-order  $\nu_6$  frequency near  $480\text{ cm}^{-1}$ , in reasonable agreement with predicted harmonic  $\pi_x$  and  $\pi_y$  frequencies ( $433\text{ cm}^{-1}$  and  $465\text{ cm}^{-1}$ ), although the present assignment implies a larger Renner-Teller splitting in this mode than suggested from our calculations. The preponderance of the SiCC bend in the CCC bend emission spectrum probably results from mode mixing upon excitation (i.e., Duschinsky mixing).

Table I summarizes the calculated and observed band origins for  $\text{SiC}_3\text{H} - \text{SiC}_5\text{H}$ , in addition to preliminary calculations on  $\text{SiC}_6\text{H}$ . The experimentally determined band origin position for  $\text{SiC}_3\text{H}$  is 1.83 eV. The  $\text{SiC}_3\text{H}$  vertical CCSD  $1^2\Sigma^+$  excited state over-estimates this excitation (2.19 eV) by 0.18 eV. The adiabatic CCSD excited state is much closer at 2.04 eV while the zero-point corrected adiabatic excitation energy (ZPE-CCSD) actually increases the excitation energy to 2.08 eV. The ZPE increase is simply a consequence of the predicted increase in the excited state vibrational frequencies; while this increase is indeed borne out for all of the assigned modes, it is probably an artifact for the highest frequency modes (particularly the CH stretch), which one would expect to be largely unaffected by electronic excitation within the Si–C moiety. The vertical CC3 computation gives a transition energy closest (within 0.15 eV) to the experimental value, probably owing to the inclusion of triples, which provides for a better description of the excitation.<sup>38</sup> The agreement between the experimental and theoretical vibrational frequencies is generally good for both the ground and excited states, with the exception of  $\nu_5$ . While it is possible to assign combination bands involving this mode and  $\nu_7$ , these assignments should be considered somewhat tentative, and may require higher resolution study to confirm their association with the  $1^2\Sigma$  state of  $l\text{-SiC}_3\text{H}$ .

## 2. Microwave data

For an appreciably polar (calculated  $\mu = 0.77\text{ D}^6$ ) radical such as  $\text{SiC}_3\text{H}$ , it is surprising that optical detection precedes microwave detection. However, earlier searches for  $l\text{-SiC}_3\text{H}$ , under experimental conditions which favored the production

TABLE V. Experimental and theoretical harmonic vibrational frequencies (in  $\text{cm}^{-1}$ ) of the ground ( $^2\Pi$ ) and first excited ( $^2\Sigma$ ) states of  $\text{SiC}_3\text{H}$ . Experimental bending frequencies in the ground state are given for the lowest Renner-Teller component.

Mode	Ground			Excited		
	Description	Calc.	Expt.	Description	Calc.	Expt.
$\nu_1$	$\sigma (a_1)$ C1–H stretch	3463		$\sigma$ C1–H stretch	3477	
$\nu_2$	$\sigma (a_1)$ C2–C1 stretch	2016		$\sigma$ C2–C1 stretch	2191	
$\nu_3$	$\sigma (a_1)$ C2–C3 stretch	1442		$\sigma$ C2–C3 stretch	1491	1492
$\nu_4$	$\sigma (a_1)$ Si–C3 stretch	632	627	$\sigma$ Si–C3 stretch	683	672
$\nu_5$	$\pi (b_1)$ C2–C1–H bend	655		$\pi (b_2)$ C2–C1–H bend	635	723
	$\pi (b_2)$ C2–C1–H bend	521		$\pi (b_1)$ C2–C1–H bend		
$\nu_6$	$\pi (b_2)$ C3–C2–C1 bend	465		$\pi (b_1)$ C3–C2–C1 bend	514	483
	$\pi (b_1)$ C3–C2–C1 bend	433	422	$\pi (b_2)$ C3–C2–C1 bend		
$\nu_7$	$\pi (b_2)$ Si–C3–C2 bend	168		$\pi (b_1)$ Si–C3–C2 bend	208	197
	$\pi (b_1)$ Si–C3–C2 bend	153	145	$\pi (b_2)$ Si–C3–C2 bend		

of similar chains, were unsuccessful. In light of the unambiguous optical data presented here, and our new theoretical calculations of its molecular structure, a second search for the rotational spectrum of *l*- $\text{SiC}_3\text{H}$  was undertaken. Within 0.5% of our best prediction, a line with closely-spaced structure (see Fig. 4), characteristic of an open-shell molecule possessing both  $\Lambda$ -doubling and hydrogen hyperfine splitting, was observed. Subsequent chemical assays and other tests quickly confirmed that the carrier of these features requires both  $\text{SiH}_4$  and  $\text{HCCH}$ , and that the carrier is paramagnetic, as expected for  $\text{SiC}_3\text{H}$ . On the assumption that this line is the  $J = 11/2 - 9/2$  transition, searches were soon undertaken for other higher- and lower- $J$  transitions. Ultimately, five lines were observed between 13 and 34 GHz (Table VI), each separated by approximately 5.2 GHz. Using a standard effective Hamiltonian for a

molecule in an isolated  $^2\Pi$  state with hyperfine structure,<sup>50–52</sup> it was possible to determine several spectroscopic constants, including the rotational constant to high precision (Table VII). The experimental rotational constant agrees to within 0.4% with our calculation, and to better than 0.2% by scaling from  $\text{SiC}_5\text{H}$ ; other constants are in excellent agreement with those predicted from  $\text{SiC}_5\text{H}$ . Although it is not obvious why our earlier search for *l*- $\text{SiC}_3\text{H}$  was unsuccessful, several factors may have conspired to prevent detection, including a search for a lower- $J$  transition which is even more sensitive to the Zeeman effect, and the lack of a hydrocarbon precursor which is an especially good source for carbon chains with three carbon atoms.

TABLE VI. Hyperfine-split rotational transitions of  $\text{SiC}_3\text{H}$  in the  $\tilde{X}^2\Pi_{3/2}$  state.

Transition <sup>a</sup>		$elf^b$	Frequency <sup>c</sup>	O–C <sup>d</sup>
$J' \rightarrow J$	$F' \rightarrow F$	$\Lambda$ -component	(MHz)	(kHz)
2.5 → 1.5	3 → 2	<i>f</i>	13 007.447	–1.8
		<i>e</i>	13 007.454	0.3
3.5 → 2.5	4 → 3	<i>f</i>	18 210.774	–1.0
		<i>e</i>	18 210.787	2.9
	3 → 2	<i>f</i>	18 211.485	3.6
		<i>e</i>	18 211.485	–5.3
4.5 → 3.5	5 → 4	<i>f</i>	23 413.977	–4.9
		<i>e</i>	23 414.001	3.7
	4 → 3	<i>f</i>	23 414.415	–3.3
5.5 → 4.5	6 → 5	<i>e</i>	23 414.437	4.0
		<i>f</i>	28 617.128	0.9
	5 → 4	<i>e</i>	28 617.149	–0.4
		<i>f</i>	28 617.438	4.5
6.5 → 5.5	7 → 6	<i>e</i>	28 617.453	–2.6
		<i>f</i>	33 820.227	–0.7
	6 → 5	<i>e</i>	33 820.259	0.9
		<i>f</i>	33 820.461	0.3
		<i>e</i>	33 820.489	–1.8

<sup>a</sup>The coupling scheme is  $F = J + I(H)$ .

<sup>b</sup>Designation of *e* and *f* levels is based on the assumption that the lambda-type doubling constant  $q$  is negative. See Table VII.

<sup>c</sup>Estimated  $1\sigma$  measurement uncertainties are 2 kHz.

<sup>d</sup>Observed minus calculated frequencies O–C are derived from the best-fit constants in Table VII.

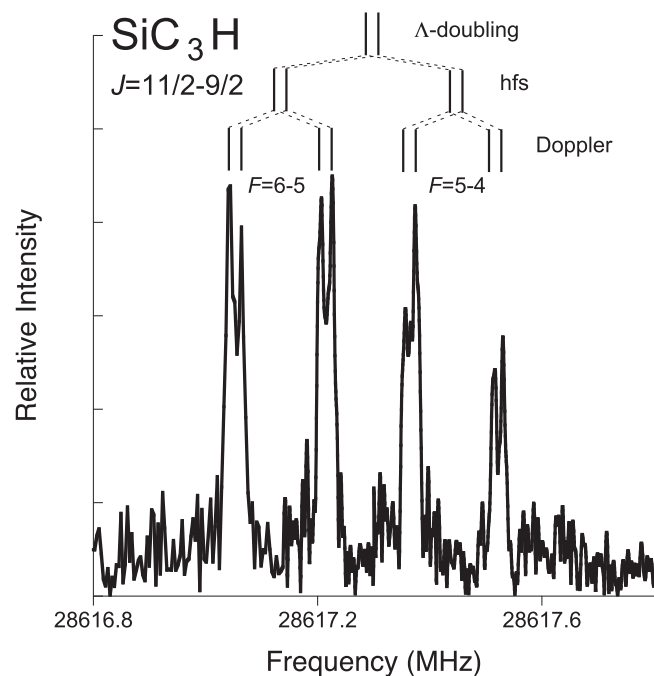
FIG. 4. The FTMW spectrum of the  $J = 11/2 - 9/2$  transition in the  $^2\Pi_{3/2}$  ground state of  $\text{SiC}_3\text{H}$  radical.

TABLE VII. Spectroscopic constants of SiC<sub>3</sub>H in the  $\tilde{X}^2\Pi_i$  state (in MHz).

Constant	Expt. <sup>a</sup>	Predicted
$A_{\text{eff}}$	1 950 000 <sup>b</sup>	...
$B$	2605.0528(3)	2610 <sup>c</sup>
$10^6 D$	209.(5)	127 <sup>d</sup>
$q$	-0.092(11) <sup>e</sup>	<0.2 <sup>f</sup>
$a + (b + c)/2$	4.9(5)	2.1 <sup>f</sup>
$b$	-41.5(10)	-30 <sup>f</sup>

<sup>a</sup>Uncertainties (in parentheses) are  $1\sigma$  in the last significant digit. Constants derived from hyperfine-split rotational transitions in Table VI.

<sup>b</sup>Derived from optical data (see text).

<sup>c</sup>Theoretical rotational constant scaled by ratio of measured value to that calculated for SiC<sub>5</sub>H.

<sup>d</sup>Value for C<sub>5</sub>H (Ref. 68).

<sup>e</sup>Sign assumed to be negative. See Ref. 68.

<sup>f</sup>From SiC<sub>3</sub>H (Ref. 5).

### C. SiC<sub>4</sub>H

The R2PI spectrum of SiC<sub>4</sub>H ( $m/z = 77$ ) is shown in Fig. 5. Owing to the low S/N ratio and large linewidths of the spectral features, as well as the wide variety of possible isomers of SiC<sub>4</sub>H,<sup>53</sup> we restrict our attention only to the coarse vibronic structure of the most conspicuous bands. In contrast to SiC<sub>3</sub>H, the spectrum shows activity in fewer vibrational modes, and significantly broader ( $>30\text{ cm}^{-1}$ ) band profiles which were found to be independent of the expansion conditions; they are therefore likely intrinsic to the radical. This behavior is qualitatively similar to that found for the isovalent chain C<sub>5</sub>H, whose optical spectrum was also observed by R2PI spectroscopy.<sup>17</sup> Although calculations indicate that the spectrum of SiC<sub>4</sub>H should be dominated by a modestly strong ( $f = 0.012$ ) transition to a  $\Pi$  electronic state with an origin near 2.8 eV, we suspect instead that the upper state is more likely the  $\Sigma$  state predicted near 2.6 eV, which the calculated  $\langle s^2 \rangle$  value indicates has predominantly quartet character. Several considerations justify such an assignment. First, the difference between the observed (2.45 eV) and predicted (3.06 eV) CC3 energy for the  $\Pi$  state seems unacceptably large in comparison to the discrepancy observed for the

$\Sigma$  states of the odd- $n$  chains ( $\leq 0.15\text{ eV}$ ). Second, the predicted  $\Pi - \Pi$  transition should be several times stronger than the observed  $\Pi - \Sigma$  transitions of SiC<sub>3</sub>H and SiC<sub>5</sub>H, yet resonant SiC<sub>4</sub>H signal was found to be nearly an order of magnitude weaker, under the same experimental conditions, and independent of the ionization wavelength. Third, the calculated geometry and frequencies for the  $\Sigma$  state indicate two acetylenic bonds, consistent with the observed spectrum (note bands at  $2038\text{ cm}^{-1}$  and  $2300\text{ cm}^{-1}$  above the origin, which have similar widths to the origin band), while the excited  $\Pi$  state is calculated to be more cumulenic, with only one acetylenic stretching frequency.

More generally, the spectrum appears qualitatively consistent with a transition to a “dark”  $\Sigma$  state which can be vibronically coupled to a brighter  $\Pi$  state. It contains three  $2000\text{ cm}^{-1}$  progressions: a short, weak one associated with the origin; a much stronger one blue-shifted from the origin by  $595\text{ cm}^{-1}$ , which shows even broader (FWHM  $> 70\text{ cm}^{-1}$ ) features; and a moderately intense one, apparently associated with the latter progression, blue-shifted by a further  $515\text{ cm}^{-1}$  and with still-broader bands, which are not built onto the origin band. It therefore seems natural to interpret the weaker  $2000\text{ cm}^{-1}$  progression as belonging to the “pure”  $\Sigma$  state, with the stronger two possibly arising from vibronic coupling to the higher-lying bright  $\Pi$  state via a  $595\text{ cm}^{-1}$  mode.

If one accepts this tentative assignment, a good candidate for the  $595\text{ cm}^{-1}$  coupling mode would be the CCC bend ( $\nu_6$ ), which is calculated to have a frequency of  $653\text{ cm}^{-1}$  in the  $\Sigma$  state. The progression blue-shifted by  $515\text{ cm}^{-1}$  would then likely correspond to the Si-C stretch, which has a predicted frequency of  $507\text{ cm}^{-1}$ , although  $2\nu_8$  ( $570\text{ cm}^{-1}$ ),  $\nu_7$  ( $464\text{ cm}^{-1}$ ), and  $\nu_4$  ( $1038\text{ cm}^{-1}$ , built onto the origin) could also contribute to the large widths of features within this progression; the complicated band profiles of the corresponding features near  $22\,950\text{ cm}^{-1}$  and  $24\,900\text{ cm}^{-1}$  suggests the presence of multiple components. Several features, including one near  $1870\text{ cm}^{-1}$ , resist obvious assignments at present. The lack of activity in the low frequency region of the spectrum makes it difficult to assign features at higher energy with confidence. Because transitions to the  $\Pi$  state likely become

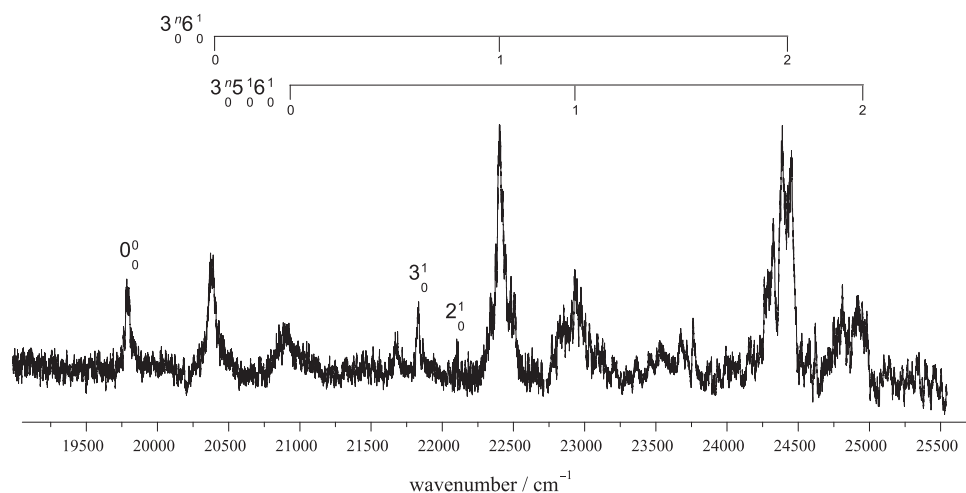


FIG. 5. R2PI spectrum of SiC<sub>4</sub>H from an acetylene-silane discharge. Assignments are for the linear isomer.

TABLE VIII. Experimental excited state band positions (in  $\text{cm}^{-1}$  relative to the origin at  $19\,803\text{ cm}^{-1}$ ) and assignments for  $l\text{-SiC}_4\text{H}$ .

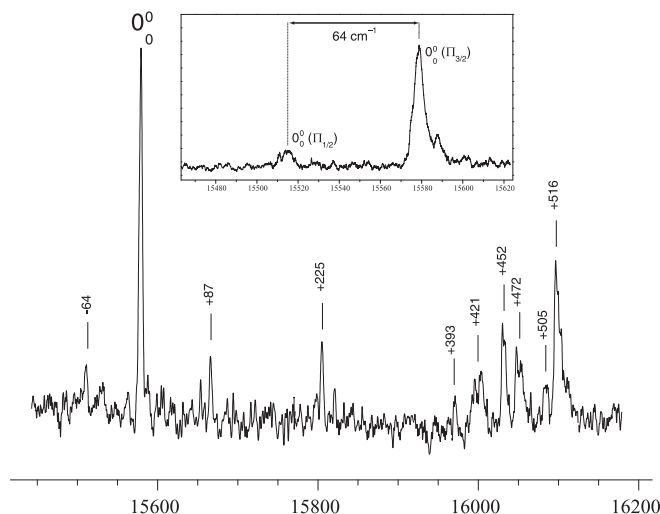
Frequency	Assignment
0	$0_0^0$
595	$6_0^1$
1113	$5_0^1 6_0^1$
1871	
2031	$3_0^1$
2300	$2_0^1$
2600	$3_0^1 6_0^1$
3130	$3_0^1 5_0^1 6_0^1$
4574	$3_0^2 6_0^1$
5101	$3_0^2 5_0^1 6_0^1$

important at higher energy, it seems imprudent to proffer a more detailed assignment of the increasingly congested region above  $\sim 23\,000\text{ cm}^{-1}$ . In addition – like  $\text{SiC}_3\text{H}$  –  $\text{SiC}_4\text{H}$  can also adopt several stable cyclic structures<sup>53</sup> which also contain optical chromophores and can be expected to have transitions within the very broad spectral range covered in our experiments.

Measured vibronic band positions and excited state frequencies based on our tentative assignments are given in Table VIII. Table IX summarizes the calculated ground and excited state frequencies for  $\text{SiC}_4\text{H}$  in addition to the experimentally determined excited state frequencies. Because of the intrinsic broadening in the spectrum, dispersed fluorescence was not attempted to measure ground state frequencies. Extremely long-lived decay of the R2PI signal from this radical suggests mixing with a quartet state (see Sec. V A).

#### D. $\text{SiC}_5\text{H}$

The spectrum of  $\text{SiC}_5\text{H}$  ( $m/z = 89$ ) is shown in Fig. 6. Only a relatively short region of the spectrum was surveyed; at increasing excitation energy, the upper state lifetime

FIG. 6. R2PI spectrum of  $\text{SiC}_5\text{H}$  from an acetylene-silane discharge, and (inset) spin-orbit separation observed for the origin band under hotter expansion conditions.

( $\sim 5\text{ ns}$ ) becomes significantly shorter than the temporal jitter of our ionization laser. Consequently, the measurement of higher vibronic bands was increasingly difficult; for the same reason, fluorescence detection was not attempted. The experimental origin for  $\text{SiC}_5\text{H}$  is  $1.93\text{ eV}$ ; as was found for  $\text{SiC}_3\text{H}$ , the vertical  $\text{CC}3$  excitation energy ( $2.07\text{ eV}$ ) gives the closest agreement with experiment for excitation to the  $1^2\Sigma^+$  state of  $\text{SiC}_5\text{H}$ . The adiabatic excitation energy for this state is  $2.12\text{ eV}$  and, as for the  $1^2\Sigma^+$  state of  $\text{SiC}_3\text{H}$ , the ZPE-corrected adiabatic CCSD excitation energy for the  $1^2\Sigma^+$  state of  $\text{SiC}_5\text{H}$  is slightly higher, owing to the predicted increase in the excited state vibrational frequencies, and thus compares less favorably with experiment.

Spectral assignments and experimental and theoretical vibrational frequencies are given in Tables X and XI. As with the  $\text{SiC}_3\text{H}$  spectrum, a Herzberg-Teller transition involving the  $\text{SiCC}$  bend ( $87\text{ cm}^{-1}$  above the origin) is apparent, while both Herzberg-Teller and Franck-Condon allowed transitions involving the lowest CCC bend are present. Our

TABLE IX. Experimental and theoretical harmonic vibrational frequencies of the lowest three electronic states of  $\text{SiC}_4\text{H}$ .

Mode	Ground ( $1^2\Pi$ )			$2\Pi$			$1\Sigma$		
	Description	Calc.		Description	Calc.	Description	Calc.	Expt.	
$\nu_1$	$\sigma (a_1)$ C1–H stretch	3469		$\sigma (a_1)$ C1–H stretch	3446	$\sigma$ C1–H stretch	3472		
$\nu_2$	$\sigma (a_1)$ C2–C1 stretch	2208		$\sigma (a_1)$ C2–C3 stretch	2099	$\sigma$ C2–C3 stretch	2266	2308	
$\nu_3$	$\sigma (a_1)$ C3–C4 stretch	2050		$\sigma (a_1)$ C3–C4 stretch	1646	$\sigma$ C3–C4 stretch	2106	2032	
$\nu_4$	$\sigma (a_1)$ C2–C3 stretch	1022		$\sigma (a_1)$ C2–C1 stretch	1098	$\sigma$ C2–C1 stretch	1038		
$\nu_5$	$\sigma (a_1)$ Si–C4 stretch	477		$\sigma (a_1)$ Si–C4 stretch	498	$\sigma$ Si–C4 stretch	508	515	
$\nu_6$	$\pi (b_2)$ C2–C1–H bend	689		$\pi (b_1)$ C2–C1–H bend	387	$\pi$ C2–C1–H bend	653	595	
	$\pi (b_1)$ C2–C1–H bend	615		$\pi (b_2)$ C2–C1–H bend	386				
$\nu_7$	$\pi (b_2)$ Carbon chain bend	522		$\pi (b_2)$ Carbon chain bend	289	$\pi$ Carbon chain bend	464		
	$\pi (b_1)$ Carbon chain bend	460		$\pi (b_1)$ Carbon chain Bend	259				
$\nu_8$	$\pi (b_1)$ Carbon chain bend	303		$\pi (b_2)$ Carbon chain bend	162	$\pi$ Carbon chain bend	285		
	$\pi (b_2)$ Carbon chain bend	264		$\pi (b_1)$ Carbon chain bend	117				
$\nu_9$	$\pi (b_1)$ Si–C4–C3 bend	112		$\pi (b_2)$ Si–C4–C3 bend	72	$\pi$ Si–C4–C3 bend	122		
	$\pi (b_2)$ Si–C4–C3 bend	93		$\pi (b_1)$ Si–C4–C3 bend	70				

TABLE X. Excited state band positions (in  $\text{cm}^{-1}$ ) and assignments for  $\text{SiC}_3\text{H}$ . Frequencies are given relative to the origin band at  $15\,579\text{ cm}^{-1}$ .

Frequency	Assignment
-64	$0_0^0 (\Sigma \leftarrow \Pi_{1/2})$
0	$0_0^0 (\Sigma \leftarrow \Pi_{3/2})$
74	
87	$11_0^1$
115	
226	$10_0^1$
242	
324	
394	$10_0^1 11_0^2$
421	$9_0^1$
452	$10_0^2$
473	$8_0^1$
506	$10_0^2 11_0^1$
516	$6_0^1$

calculations indicate that the vibronically induced transitions in this radical probably result from coupling to a higher-lying (by  $\sim 2\text{ eV}$ )  $\Pi$  state with an  $f$ -value near unity, which is also similar to that found for  $\text{SiC}_3\text{H}$ .

Because the Si-C bond is predicted to significantly shorten upon excitation, we assign the strong band at  $516\text{ cm}^{-1}$  as the Si-C stretch, which gives a frequency in good agreement with theory ( $511\text{ cm}^{-1}$ ), while moderately intense bands at  $474\text{ cm}^{-1}$  and  $426\text{ cm}^{-1}$  probably correspond to the CCC bending modes (predicted frequencies of  $518\text{ cm}^{-1}$  and  $452\text{ cm}^{-1}$ , respectively). Most of the bands in this region can subsequently be assigned to these few modes and combinations thereof; weaker bands associated with the very close-lying ( $0.03\text{ eV}$ ), dark  $\Pi$  state might arise from vibronic coupling to the brighter  $\Sigma$  state.

Under “hotter” expansion conditions – high discharge voltage, low backing pressure, reduced nozzle-skimmer distance – it was possible to enhance the relative intensity of features lying  $10\text{ cm}^{-1}$  to the blue and  $64\text{ cm}^{-1}$  to the red of the origin band (see inset in Fig. 6). While the former is probably a vibrational sequence band (several vibrational modes could cause the observed blue-shift, on the basis of our calculations) the  $64\text{ cm}^{-1}$  band is most readily interpreted as the transition from the upper spin-orbit component ( $^2\Pi_{1/2}$ ) of the ground state to the vibrationless excited state, which yields a spin-orbit splitting which is close in magnitude with that derived previously for  $\text{SiCH}$  ( $69.8\text{ cm}^{-1}$ <sup>14</sup>),  $\text{SiC}_2\text{H}$  ( $73.2\text{ cm}^{-1}$ <sup>48</sup>), and  $\text{SiC}_3\text{H}$  ( $64\text{ cm}^{-1}$ , this work). The very small variation of the spin-orbit separation with chain length suggests that the unpaired electron in these radicals resides predominantly on the silicon atom, as was suggested in the earlier rotational study.<sup>5</sup>

## V. DISCUSSION

### A. Comparison with isovalent $\text{C}_n\text{H}$ chains

For the isovalent carbon chain radicals, a roughly linear relationship between chain length and excitation wavelength has been observed both for the odd- and even- $n$  numbered chains, for electronic transitions which have the same excitation character (e.g., the transitions for the odd- $n$  chains which involve excitation from the  $\sigma$  HOMO-1 to the partially filled  $\pi$  HOMO). This behavior has been rationalized in terms of the free-electron model, whereby  $\pi$  electrons are delocalized over the length of the chain, yielding a decrease in  $T_e$  with increasing chain length. With the earlier detection of  $\text{SiCH}$  by Smith *et al.*,<sup>14</sup> and the detections of  $\text{SiC}_3\text{H}$  and  $\text{SiC}_5\text{H}$  herein, it would seem that sufficient data now exists to establish whether a similar trend occurs for the optical transitions of the odd- $n$  silicon-terminated chains. However, the electronic states of the isovalent carbon chains which correspond to the present optical transitions are not the high-lying  $\Pi$  states, but rather the nearly degenerate lowest  $\Sigma$  and  $\Pi$

TABLE XI. Experimental and theoretical harmonic vibrational frequencies (in  $\text{cm}^{-1}$ ) of the ground ( $^2\Pi$ ) and first excited ( $^2\Sigma$ ) states of  $\text{SiC}_3\text{H}$  radical.

Mode	Ground			Excited		
	Description	Calc.		Description	Calc.	Expt.
$\nu_1$	$\sigma (a_1)$ C1-H stretch	3469		$\sigma$ C1-H stretch	3475	
$\nu_2$	$\sigma (a_1)$ C2-C1 stretch	2157		$\sigma$ C3-C2 stretch	2349	
$\nu_3$	$\sigma (a_1)$ C3-C4 stretch	2029		$\sigma$ C2-C1 stretch	2161	
$\nu_4$	$\sigma (a_1)$ C4-C5 stretch	1548		$\sigma$ C4-C5 stretch	1541	
$\nu_5$	$\sigma (a_1)$ C3-C2-Stretch	971		$\sigma$ C3-C4 stretch	1014	
$\nu_6$	$\sigma (a_1)$ Si-C5 stretch	487		$\sigma$ Si-C5 stretch	509	516
$\nu_7$	$\pi (b_1)$ C2-C1-H bend	676		$\pi$ C2-C1-H bend	651	
	$\pi (b_2)$ C2-C1-H bend	604				
$\nu_8$	$\pi (b_1)$ Carbon chain bend	515		$\pi$ Carbon chain bend	518	473
	$\pi (b_2)$ Carbon chain bend	497				
$\nu_9$	$\pi (b_2)$ Carbon chain bend	430		$\pi$ Carbon chain bend	452	418
	$\pi (b_1)$ Carbon chain bend	398				
$\nu_{10}$	$\pi (b_1)$ Carbon chain bend	203		$\pi$ Carbon chain bend	245	226
	$\pi (b_2)$ Carbon chain bend	203				
$\nu_{11}$	$\pi (b_1)$ Si-C5-C4 bend	75		$\pi$ Si-C5-C4 bend	98	87
	$\pi (b_2)$ Si-C5-C4 bend	74				

states. The energy separation of these states ( $\Sigma$  minus  $\Pi$ ) for the chains  $C_{2n}H$  ( $n = 1 - 3$ ) is, respectively,  $-0.45$  eV,<sup>15</sup>  $0.026$  eV,<sup>48</sup> and  $0.181$  eV.<sup>47</sup> The  $\Sigma$  states can be generated by removing an electron from a non-bonding orbital on the terminal carbon and placing it in the highest occupied  $\pi$  orbital, which is a bonding orbital. Consequently, the terminal C–C bond significantly shortens in the  $\Sigma$  state,<sup>54</sup> approaching the acetylenic value of  $1.21$  Å.

In contrast to the  $C_{2n}H$  chains, which have closely spaced electronic ground states of  $\Sigma$  or  $\Pi$  symmetry, the ground electronic states of  $SiC_{2n+1}H$  always have  $\Pi$  symmetry, and they are well-separated from the excited  $\Sigma$  states. This is due to unfavourable hybridization of the Si  $3s$  and  $3p$  orbitals in comparison to the carbon  $2s$  and  $2p$  orbitals,<sup>55</sup> which raises the energy of the highest partially filled, bonding  $\pi$  HOMO relative to the fully occupied, non-bonding  $\sigma$  MO centered on silicon. Nevertheless, the electronic configurations of the excited  $\Sigma$  states in the silicon-terminated chains are analogous to those of the low-lying  $\Sigma$  states of the isovalent carbon chains. The first excited  $\Sigma$  states arise from promotion of an electron in a  $\sigma$  non-bonding MO into the highest-lying partially occupied  $\Pi$  MO. In  $SiC_3H$ , this corresponds to excitation from the HOMO-1 to the HOMO, while for  $SiC_5H$ , it is a HOMO  $\leftarrow$  HOMO-2 transition. As for the  $C_nH$  analogues, the highest  $\sigma$  MO continues to drop in energy relative to the partially filled  $\pi$  orbital with increasing chain length, shifting the  $\Sigma \leftarrow \Pi$  transition further to the blue (we predict a vertical transition near  $2.5$  eV for  $SiC_7H$ ). The calculations indicate that this transition should produce a rare SiC triple bond (length  $\approx 1.61$  Å), which is borne out by the available experimental evidence. Analysis of the rotationally resolved SiCH electronic spectrum by Smith *et al.*<sup>14</sup> gave ground and excited state SiC bond lengths of  $1.693$  Å, and  $1.612$  Å, respectively;<sup>14</sup> while for  $SiC_3H$ , our LIF and DF spectra suggests that the Si–C stretching frequency increases significantly upon electronic excitation, from  $630$   $cm^{-1}$  to  $672$   $cm^{-1}$ . That the triply-bonded states of these species lie several tens of kcal/mol above the doubly-bonded ground states underscores the well-known reluctance of silicon to form multiple bonds.

The main difference between the optical spectra of the two  $C_nH$  “families” – specifically, that the spectra of the odd- $n$  chains are intrinsically broadened,<sup>17</sup> while those of the even- $n$  chains (for chains shorter than  $C_8H$ ) are sharp – persists also for their silicon-terminated analogues. Intrinsic broadening in the optical spectra of carbon chain radicals has been ascribed to internal conversion, owing to a high density of vibrational states in the ground electronic state;<sup>56</sup> vibronic coupling between low-lying  $\Sigma$  and  $\Pi$  states, particularly for longer chains (e.g.,  $C_8H$ <sup>57</sup>); and to intersystem crossing.<sup>58</sup> While the upper state lifetime for the odd- $n$  chains indeed decreases with chain length (from  $100$  ns to  $10$  ns), the “lifetime” that we infer from intrinsic broadening in the  $SiC_4H$  spectrum – approx.  $100$  fs – would seem to suggest a different relaxation mechanism. Because the first excited  $\Sigma$  states of all the species studied herein are all well-separated from the  $\Pi$  ground electronic states, it is not obvious why internal conversion should not be similarly persistent for both odd- $n$  and even- $n$  chains.

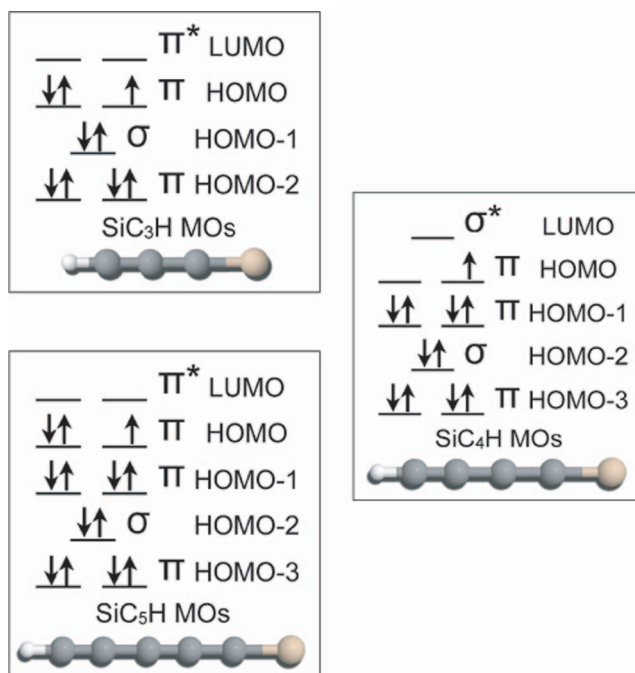


FIG. 7. Frontier orbital occupancies for the linear isomers of  $SiC_3H$ ,  $SiC_4H$ , and  $SiC_5H$ .

Rather, we believe that intersystem crossing is the dominant broadening mechanism in the  $SiC_4H$  spectrum, and likely takes place in other members of the series. Figure 7 shows schematic electronic configurations which apply for the odd- $n$  (left) and even- $n$  (right)  $SiC_nH$  chains. For the odd- $n$  chains, the lowest quartet state arises from promotion of an electron in the  $\pi$ -bonding HOMO into the anti-bonding LUMO. The HOMO-LUMO gap in these species lies in the near UV, significantly higher than the lowest  $\Sigma$  states. In contrast, for the even- $n$  chains, the first excited  $\Sigma$  ( $\sigma$  HOMO-2 to the  $\pi$  HOMO) and  $\Pi$  ( $\pi$  HOMO-1 to the  $\pi$  HOMO) states are both generated from excitations within bonding MOs, and can give rise to quartets with similar energies; consequently, the potential for doublet-quartet mixing is significantly increased in these systems relative to the odd- $n$  chains. The excited state relaxation dynamics of  $SiC_4H$  were probed in R2PI by delaying the ionizing photon relative to the resonant photon. Even with a delay of  $50$   $\mu s$  (the longest delay possible with our detection geometry, because species in longer-lived states exit the extraction region), no significant decay in resonant signal was observed. The lifetime broadening in the spectrum can be reconciled with the very long excited state lifetime inferred from our experimental timings by noting that former can arise from rapid crossing to a nearby quartet state following electronic excitation, while the latter is due to subsequent slow, spin-forbidden decay to the ground state.

## B. Longer chains, nonlinear isomers, and prospects for interstellar detection

In anticipation of optical detection, calculations were also performed on the ground and first two excited states of  $SiC_6H$ . The electronic spectrum of this species is expected to be similar to that of  $SiC_4H$ , with analogous transitions to a dark  $\Sigma$

state ( $f = 10^{-5}$ ) and a nearby bright  $\Pi$  state ( $f = 0.015$ ) predicted near 2.6 eV. However, while this species was readily detected in the rotational band, searches for its optical spectrum were unsuccessful. Renewed searches for this and still longer chains in a jet-cooled discharge may be feasible using diacetylene as a precursor, as was found for the earlier microwave measurements. While the even- $n$   $\text{SiC}_n\text{H}$  chains should be detectable by R2PI through ionization from long-lived quartet states, increasingly rapid internal conversion of the excited states of odd- $n$  chains – the isovalent chain  $\text{C}_8\text{H}$  has an inferred lifetime of 8 ps<sup>57</sup> – may necessitate detection of longer members of the series by cavity-ringdown spectroscopy.

All of the electronic transitions reported herein for the  $\text{SiC}_n\text{H}$  radicals lie in the DIB region, but these transitions (i.e., to the first excited states) are almost certainly too weak to merit consideration in connection with this longstanding unsolved mystery. However, these chains are predicted to have extraordinarily strong ( $f \approx 1$ )  $\pi^* \leftarrow \pi$  transitions; while these transitions lie deep in the UV for  $\text{SiC}_3\text{H}$  (5.36 eV) and  $\text{SiC}_5\text{H}$  (4.91 eV), they should enter the DIB region for longer chains. If one also considers the analogous transition of  $\text{SiC}_7\text{H}$  (predicted at 4.46 eV with  $f = 0.82$ ), there is a clear linear decrease in the transition energy as a function of the number of carbon atoms, as expected from the free-electron model. On the basis of this linear trend, the shortest chain whose strong  $3\Pi \leftarrow 1^2\Pi$  transition overlaps the DIB region will have to contain at least 13 carbon atoms. While such long silicon-containing chains are unlikely to be highly abundant in space, the strength of these transitions is encouraging and warrants their investigation in the laboratory.

Multiple low-lying cyclic structures are possible for  $\text{SiC}_n\text{H}$  where  $n \geq 2$ .<sup>6,54,59,60</sup> Of particular interest are those isomers which are structurally similar to interstellar  $c\text{-SiC}_2$  and rhomboidal  $\text{SiC}_3$ . The former species is so abundant in IRC+10216 that several of its rare silicon isotopologues have been detected;<sup>61</sup> it is also the carrier of the well-known blue-green Merrill-Sanford bands observed in emission in carbon stars.<sup>62</sup> For  $\text{SiC}_3$ , one chain and two rhomboidal forms have been detected in the laboratory,<sup>8,9</sup> and one of them so far in space.<sup>63</sup> Several quite stable isomers of  $\text{SiC}_3\text{H}$  and  $\text{SiC}_4\text{H}$  incorporating all three motifs have been predicted<sup>6,54</sup> to lie within only 85 kcal/mol of the linear ground states – similar to the energy difference between HNC, HONC, and HCNO, all of which have now been detected in the laboratory and in space.<sup>7,64–67</sup>

Ring-containing  $\text{SiC}_n\text{H}$  species may also possess electronic transitions in the visible because they contain at least one optical chromophore (e.g.,  $c\text{-SiC}_2$ , and carbon chain moieties  $\text{C}_3\text{H}$  and  $\text{C}_4\text{H}$ ). Indeed, there is some evidence to suggest the presence of a ring-containing isomer in our  $\text{SiC}_3\text{H}$  spectrum (see Fig. 1). There remain three weak bands designated with asterisks—at 1046, 1132, and 1383  $\text{cm}^{-1}$  above the origin. Our ROHF-EOM-CCSD/aug-cc-pVTZ calculations on the isomer designated F1 by Sun *et al.*,<sup>6</sup> which is similar in structure to the rhomboidal  $\text{SiC}_3$  isomer that contains a transannular Si–C bond<sup>9</sup> (see Fig. 8), indicate an  $A'$  ground state only 6.9 kcal/mol above the linear ground state, and a vertical transition to an excited  $A'$  state with  $f$ -value (0.003

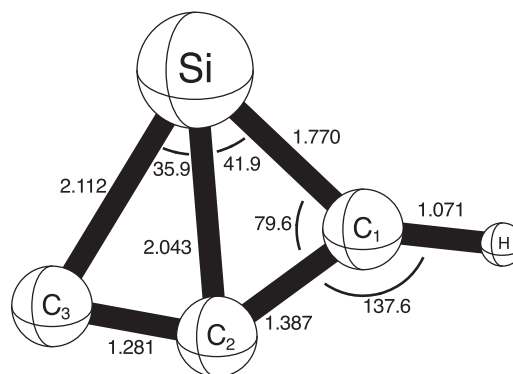


FIG. 8. A cyclic isomer of  $\text{SiC}_3\text{H}$ , predicted to lie only 7 kcal/mol above the linear ground state, and which has a moderately intense transition near 2 eV. The rhomboidal  $\text{SiC}_3$  moiety is similar in structure to one of the two known rhomboidal forms of  $\text{SiC}_3$ .<sup>9</sup>

at 2.06 eV) very similar to that of the observed  $\Sigma$  state. If one tentatively assigns the lowest “unexplained” band (at 1046  $\text{cm}^{-1}$  above the  $l\text{-SiC}_3\text{H}$  origin) as the origin transition of this isomer, the other unassigned features correspond to vibrational energies of 85  $\text{cm}^{-1}$  and 340  $\text{cm}^{-1}$ , both of which can plausibly be assigned as  $7_0^1$  (95  $\text{cm}^{-1}$ , predicted for the lowest  $a'$  mode) and  $9_0^2$  (370  $\text{cm}^{-1}$ , for 2 quanta of the lowest  $a''$  mode); most of the higher frequency modes fall outside the range of our scan. Regrettably, these bands were too weak under our experimental conditions for meaningful DF spectra to be recorded; our hypothesis might be better tested by visible-visible hole-burning spectroscopy. It will also be of interest to detect the rotational spectra of this and other nonlinear isomers: the laboratory and astronomical detection of related  $\text{SiC}_3$  isomers augurs well for their detection in the rotational band; additionally, because they are predicted to have significantly larger dipole moments than the linear isomers,<sup>6,54</sup> ring-containing species may be good targets for future searches in the radio band, either in the laboratory, in space, or both.

## VI. CONCLUSION

The gas-phase optical detection and characterization of the silicon-terminated carbon chains  $\text{SiC}_n\text{H}$  ( $n = 3 - 5$ ) has been carried out, as has the rotational detection of the missing member of the series,  $\text{SiC}_3\text{H}$ . Coupled cluster calculations indicate that, for the odd- $n$  chains, the transitions are dominated by excitation to a  $^2\Sigma$  state which is vibronically coupled to a higher-lying  $\Pi$  state; while for  $\text{SiC}_4\text{H}$ , the observed excited state appears to be strongly mixed with a quartet state, as evidenced by its long-lifetime (significantly longer than 50  $\mu\text{s}$ ) determined by R2PI spectroscopy. The lowest  $^2\Sigma$  states of the odd- $n$  chains, which lie approximately 2 eV above ground, are analogues of the very low-lying  $\Sigma$  states of the isovalent  $\text{C}_n\text{H}$  chains: both theory and experiment suggest that these states are characterized by a rare Si–C triple bond (with a predicted length of 1.61 Å), which was observed previously for the excited  $\Sigma$  state of  $\text{SiCH}$ . Transitions to the first excited states in all chains are too weak to be astronomically important; however, extremely strong transitions (with  $f$ -values near unity) are predicted for the odd- $n$  chains, and should overlap the DIB

region for chains containing 13 or more carbon atoms. The best prospects for the astronomical detection of the silicon-terminated carbon chain radicals of intermediate size appear to lie in the rotational band, for which accurate rest frequencies are now in hand for  $n = 2 - 6$ . Because the  $\text{SiC}_3\text{H}$  optical spectrum suggests the presence of multiple isomers, further investigation at rotational resolution or by visible-visible hole-burning spectroscopy is warranted.

## ACKNOWLEDGMENTS

The work in Cambridge is supported by NSF Grant No. CHE-1058063 and NASA Grant No. NNX13AE59G. Support for T.D.C. and R.C.F. is provided by the U.S. National Science Foundation Award No. CHE-1058420 and by Award No. CHE-0741927 (T.D.C.): a Multi-User Chemistry Research Instrumentation and Facility (CRIF:MU). The molecular structures in Fig. 7 were generated with the JMOL program, and Fig. 8 was generated with the CheMVP program developed at the Center for Computational and Quantum Chemistry at the University of Georgia. R.C.F. also wishes to thank the Virginia Space Grant Consortium for a Graduate Research Fellowship part of which was allocated during the time of this research. The authors would like to thank John Stanton for helpful discussions of this work.

- <sup>1</sup>P. Thaddeus and M. C. McCarthy, *Spectrochim. Acta A* **57**, 757 (2001).
- <sup>2</sup>H. Gupta, C. A. Gottlieb, M. C. McCarthy, and P. Thaddeus, *Astrophys. J.* **691**, 1494 (2009).
- <sup>3</sup>G. H. Herbig, *Annu. Rev. Astron. Astrophys.* **33**, 19 (1995).
- <sup>4</sup>C. A. Rice and J. P. Maier, *J. Phys. Chem. A* **117**, 5559 (2013).
- <sup>5</sup>M. C. McCarthy, A. J. Apponi, C. A. Gottlieb, and P. Thaddeus, *J. Chem. Phys.* **115**, 870 (2001).
- <sup>6</sup>H. Sun, N. Tan, H. Q. He, X. M. Pan, Z. M. Su, and R. S. Wang, *Theor. Chem. Acc.* **119**, 501 (2008).
- <sup>7</sup>M. Mladenovic, M. Lewerenz, M. C. McCarthy, and P. Thaddeus, *J. Chem. Phys.* **131**, 174308 (2009).
- <sup>8</sup>M. C. McCarthy, A. J. Apponi, and P. Thaddeus, *J. Chem. Phys.* **110**, 10645 (1999).
- <sup>9</sup>M. C. McCarthy, A. J. Apponi, and P. Thaddeus, *J. Chem. Phys.* **111**, 7175 (1999).
- <sup>10</sup>E. B. Jochnowitz and J. P. Maier, *Ann. Rev. Phys. Chem.* **59**, 519 (2008).
- <sup>11</sup>K. Hoshina, H. Kohguchi, Y. Ohshima, and Y. Endo, *J. Chem. Phys.* **108**, 3465 (1998).
- <sup>12</sup>H. Linnartz, T. Motylewski, O. Vaizert, J. P. Maier, A. J. Apponi, M. C. McCarthy, C. A. Gottlieb, and P. Thaddeus, *J. Mol. Spectrosc.* **197**, 1 (1999).
- <sup>13</sup>M. V. R. Cireasa and D. Cossart, *Eur. Phys. J. D* **2**, 199 (1998).
- <sup>14</sup>T. C. Smith, H. Y. Li, D. J. Clouthier, C. T. Kingston, and A. J. Merer, *J. Chem. Phys.* **112**, 3662 (2000).
- <sup>15</sup>P. G. Carrick, A. J. Merer, and R. F. Curl, *J. Chem. Phys.* **78**, 3652 (1983).
- <sup>16</sup>F. J. Mazzotti, R. Raghunandan, A. M. Esmail, M. Tulej, and J. P. Maier, *J. Chem. Phys.* **134**, 164303 (2011).
- <sup>17</sup>H. Ding, T. Pino, F. Güthe, and J. P. Maier, *J. Chem. Phys.* **117**, 8362–8367 (2002).
- <sup>18</sup>J. G. Phillips and S. P. Davis, "The Swan system of the  $\text{C}_2$  molecule," *The Berkeley Analysis of Molecular Spectra* (University of California Press, Berkeley, CA, 1968).
- <sup>19</sup>K. S. Ojha and R. Gopal, *Spectrochim. Acta A* **71**, 1003 (2008).
- <sup>20</sup>K. Raghavachari, G. W. Trucks, J. A. Pople, and M. Head-Gordon, *Chem. Phys. Lett.* **157**, 479 (1989).
- <sup>21</sup>J. Gauss, J. F. Stanton, and R. J. Bartlett, *J. Chem. Phys.* **95**, 2623 (1991).
- <sup>22</sup>J. D. Watts, J. Gauss, and R. J. Bartlett, *Chem. Phys. Lett.* **200**, 1 (1992).
- <sup>23</sup>T. H. Dunning, *J. Chem. Phys.* **90**, 1007 (1989).
- <sup>24</sup>K. A. Peterson and T. H. Dunning, *J. Chem. Phys.* **102**, 2032 (1995).
- <sup>25</sup>T. H. Dunning, K. A. Peterson, and A. K. Wilson, *J. Chem. Phys.* **114**, 9244 (2001).
- <sup>26</sup>I. Shavitt and R. J. Bartlett, *Many-Body Methods in Chemistry and Physics: MBPT and Coupled-Cluster Theory* (Cambridge University Press, Cambridge, 2009).
- <sup>27</sup>H. Koch, O. Christiansen, P. Jørgensen, A. M. S. de Merás, and T. Helgaker, *J. Chem. Phys.* **106**, 1808 (1997).
- <sup>28</sup>O. Christiansen, H. Koch, and P. Jørgensen, *J. Chem. Phys.* **103**, 7429 (1995).
- <sup>29</sup>K. Hald, P. Jørgensen, O. Christiansen, and H. Koch, *J. Chem. Phys.* **116**, 5963 (2002).
- <sup>30</sup>C. E. Smith, R. A. King, and T. D. Crawford, *J. Chem. Phys.* **122**, 054110 (2005).
- <sup>31</sup>J. F. Stanton and R. J. Bartlett, *J. Chem. Phys.* **98**, 7029 (1993).
- <sup>32</sup>A. I. Krylov, *Ann. Rev. Phys. Chem.* **59**, 433 (2008).
- <sup>33</sup>R. A. Kendall, T. H. Dunning, and R. J. Harrison, *J. Chem. Phys.* **96**, 6796 (1992).
- <sup>34</sup>J. S. Binkley, J. A. Pople, and P. S. Dobosh, *Mol. Phys.* **28**, 1423 (1974).
- <sup>35</sup>J. Gauss, W. J. Lauderdale, J. F. Stanton, J. D. Watts, and R. J. Bartlett, *Chem. Phys. Lett.* **182**, 207 (1991).
- <sup>36</sup>W. J. Lauderdale, J. F. Stanton, J. Gauss, J. D. Watts, and R. J. Bartlett, *Chem. Phys. Lett.* **187**, 21 (1991).
- <sup>37</sup>J. D. Watts, J. Gauss, and R. J. Bartlett, *J. Chem. Phys.* **98**, 8718 (1993).
- <sup>38</sup>R. C. Fortenberry, R. A. King, J. F. Stanton, and T. D. Crawford, *J. Chem. Phys.* **132**, 144303 (2010).
- <sup>39</sup>R. C. Fortenberry and T. D. Crawford, *J. Chem. Phys.* **134**, 154304 (2011).
- <sup>40</sup>R. C. Fortenberry and T. D. Crawford, *J. Phys. Chem. A* **115**, 8119 (2011).
- <sup>41</sup>R. C. Fortenberry, *Mol. Phys.* **111**, 3265 (2013).
- <sup>42</sup>R. C. Fortenberry and T. D. Crawford, *Annu. Rep. Comput. Chem.* **7**, 195 (2011).
- <sup>43</sup>T. D. Crawford, C. D. Sherrill, E. F. Valeev, J. T. Fermann, R. A. King, M. L. Leininger, S. T. Brown, C. L. Janssen, J. P. Kenny, E. T. Seidl, and W. D. Allen, *J. Comput. Chem.* **28**, 1610 (2007).
- <sup>44</sup>CFOUR, a quantum chemical program package written by J. F. Stanton, J. Gauss, M. E. Harding, P. G. Szalay with contributions from A. A. Auer *et al.* For the current version, see <http://www.cfour.de>.
- <sup>45</sup>J. P. Maier, *J. Phys. Chem.* **102**, 3462 (1998).
- <sup>46</sup>T. R. Taylor, C. S. Xu, and D. M. Neumark, *J. Chem. Phys.* **108**, 10018 (1998).
- <sup>47</sup>J. Zhou, E. Garand, and D. M. Neumark, *J. Chem. Phys.* **127**, 154320 (2007).
- <sup>48</sup>A. J. Apponi, M. C. McCarthy, C. A. Gottlieb, and P. Thaddeus, *Astrophys. J.* **536**, L55 (2000).
- <sup>49</sup>J. T. Hougen, *J. Chem. Phys.* **36**, 519 (1962).
- <sup>50</sup>J. Brown, M. Kaise, C. Kerr, and D. Milton, *Mol. Phys.* **36**, 553 (1978).
- <sup>51</sup>J. Brown, E. Colbourn, J. Watson, and F. Wayne, *J. Mol. Spectrosc.* **74**, 294 (1979).
- <sup>52</sup>C. Amiot, J.-P. Maillard, and J. Chauville, *J. Mol. Spectrosc.* **87**, 196 (1981).
- <sup>53</sup>H.-Y. Zhao, L. Wang, J. Li, Y. Liu, Y.-C. Li, and S.-L. Qin, *Comput. Theor. Chem.* **994**, 19 (2012).
- <sup>54</sup>D. E. Woon, *Chem. Phys. Lett.* **244**, 45 (1995).
- <sup>55</sup>W. Kutzelnigg, *Angew. Chem., Int. Ed.* **23**, 272 (1984).
- <sup>56</sup>H. Kohguchi, Y. Ohshima, and Y. Endo, *Chem. Phys. Lett.* **254**, 397 (1996).
- <sup>57</sup>P. Birza, D. Khoroshev, A. Chirokolava, T. Motylewski, and J. P. Maier, *Chem. Phys. Lett.* **382**, 245 (2003).
- <sup>58</sup>A. E. Boguslavskiy and J. P. Maier, *J. Chem. Phys.* **125**, 094308 (2006).
- <sup>59</sup>J. R. Flores, *Chem. Phys. Lett.* **392**, 196 (2004).
- <sup>60</sup>D. Han, C. M. L. Rittby, and W. R. M. Graham, *J. Chem. Phys.* **106**, 6222 (1997).
- <sup>61</sup>D. L. Kokkin, S. Brünken, K. H. Young, N. A. Patel, C. A. Gottlieb, P. Thaddeus, and M. C. McCarthy, *Astrophys. J., Suppl. Ser.* **196**, 17 (2011).
- <sup>62</sup>P. J. Sarre, M. E. Hurst, and T. L. Evans, *Mon. Not. R. Astron. Soc.* **319**, 103 (2000).
- <sup>63</sup>A. J. Apponi, M. C. McCarthy, C. A. Gottlieb, and P. Thaddeus, *Astrophys. J.* **516**, L103 (1999).
- <sup>64</sup>W. H. Hocking, M. C. L. Gerry, and G. Winnewisser, *Astrophys. J.* **174**, L93 (1972).
- <sup>65</sup>L. E. Snyder and D. Buhl, *Astrophys. J.* **177**, 619 (1972).
- <sup>66</sup>M. Winnewisser and B. P. Winnewisser, *Z. Naturforsch.* **26a**, 128 (1971).
- <sup>67</sup>N. Marcelino, J. Cernicharo, B. Tercero, and E. Roueff, *Astrophys. J.* **690**, L27 (2009).
- <sup>68</sup>M. C. McCarthy, W. Chen, A. J. Apponi, C. A. Gottlieb, and P. Thaddeus, *Astrophys. J.* **520**, 158 (1999).